Evolution of Composite Defects during Manufacturing: Wrinkles & Delamination

Sandeep Chava[1], Sirish Namilae[2]

[1]PhD Student, [2]Associate Professor, Department of Aerospace Engineering
Embry-Riddle Aeronautical University
Daytona Beach, Florida/USA

ABSTRACT

The ubiquitous usage of polymer matrix composites in many applications demands a comprehensive understanding of composite interfaces, which critically affect both the manufacturing processes and the deformation mechanisms. Processing-induced defects in composite structures such as wrinkles and delaminations are primarily a result of inter-ply interfacial movement during manufacturing. In this paper, a new in-situ experimental approach and an ex-situ X-Ray characterization are proposed for developing a fundamental understanding of ply interfaces during composite manufacturing. A carbon fiber laminate is cured in a specially designed autoclave with viewports with plies laid-up on a mold with cylindrical tooling setup to simulate the maximum movement of plies, resulting in the formation of wrinkles and delamination. Three cylindrical tools of radius 9.5mm, 12.7mm and 15.9mm are used in preparing three different molds for the layup. Ply-movement is measured in-situ using Digital Image Correlation (DIC) during the cure cycle through the viewports of the autoclave. In addition, the resulting defects are characterized post-cure using X-Ray Micro-CT. Results show that at wrinkle the maximum out-of-plane movement of 1.32 mm is happening for a 4-ply unidirectional laminate laid up on a mold with 15.9mm tool diameter.

1. INTRODUCTION

The pervasive usage of polymer matrix composites in aerospace [1], automobile [2], and other applications [3] necessitates a comprehensive understanding of composite interfaces that critically affect both the manufacturing processes and the deformation mechanisms in composites. Interfaces are two-dimensional transition regions in materials and are typically associated with higher entropy [4]. Because of this higher energy state, interfaces not only exhibit increased chemical activity [4, 5] but also play a key role in limiting deformation processes (e.g., fracture) [6-8]. This is especially true in composites where two dissimilar materials interact, for example, load transfer to fibers and hence the mechanical behavior of composites is essentially defined by the well-studied fiber-matrix interface [6-9]. A relatively less studied aspect of the composite interfacial behavior is that of the evolution of the inter-ply interfaces during the manufacturing of aerospace composites. Effective chemical bonding at these interfaces during fabrication would result in a defect-free structure, while the movement of these ply interfaces leads to processing induced defects, including porosity, wrinkles, and delaminations.

As shown in the schematic in figure 1, defects such as porosity, debonding, voids, resin affluent areas, foreign objects, broken fibers, wrinkling, matrix cracking, delamination, and blisters are observed during composite processing [10]. Defects like delaminations and wrinkling which are associated with the interfacial ply movement are common defects in composite manufacturing. Manufacturing companies like Boeing [11] and Airbus[12] have suffered substantial economic impacts due to these processing-induced defects in the manufacturing of airplane parts in the past. Inter-ply friction and slippage are identified as responsible for both delamination and wrinkles. This can either be observed in the manufacturing of parts with curvature or while trying to achieve a specific shape by creating a mold with a foreign object underneath plies [13].

In this context, it is essential to understand the evolution of the interfaces between plies and related processing defects like wrinkles and delaminations. Consider wrinkles for example; they are studied in various fields such as skin wrinkles [14], thin films [15], sheet metal forming [16], and fabrics [17], consequently theoretical developments such as scaling behavior [18], kinematic and geometric modeling [19], shear locking behavior [20], etc. can be applied to composite wrinkles. Processing-induced delamination and wrinkling are closely related. Inter-ply shear deformation and restricted motion are responsible for wrinkles, while inter-ply interface displacement in the normal direction causes delaminations. The formation of both of these defects, as well as other processing-induced defects, are primarily defined by the inter-ply adhesion and slip behavior in response to the processing conditions

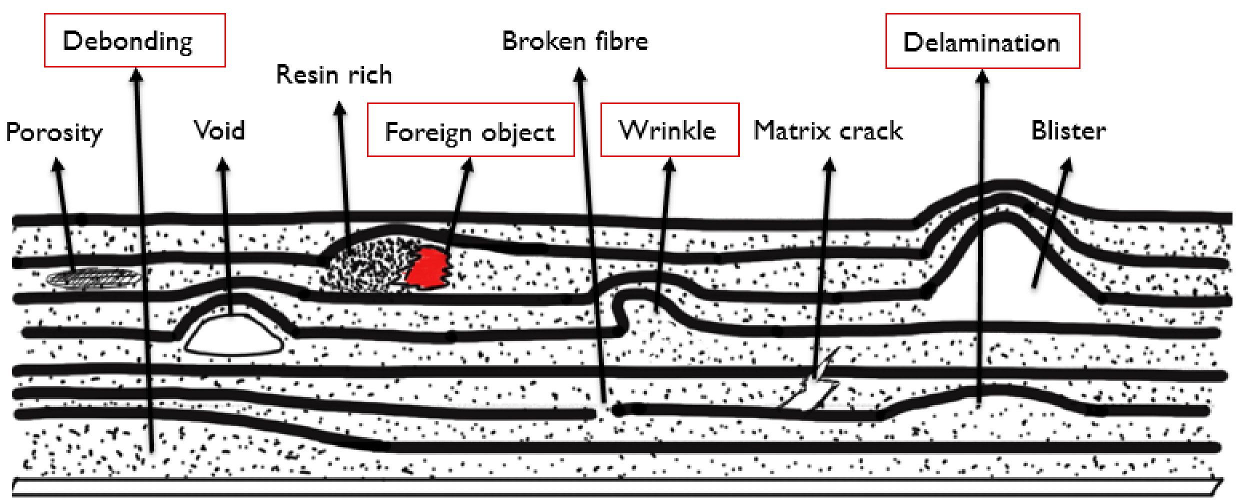

Figure 1. Schematic of ply layup showing all the defects in composites.

Published studies from literature focused on the effect of these manufacturing defects in reducing both the strength and the stiffness of the composite structures [21]. Some of the studies predicted and analyzed the formation of some of the processing-induced defects [22]. Despite these studies, there is a further need to understand the fundamental behavior of ply interfaces to engineer methods that reduce the occurrence of processing-induced defects like wrinkles and delamination. This inter-ply behavior depends on both the evolution of chemical crosslinking between partially cured polymer layers at the interface and the interfacial response to the thermomechanical loads during processing. In many cases, a design requirement like double curvature of the molds [23] can lead to these defects. Many of these studies are applied to the composite structure post-manufacturing. Current research focusses on identifying the conditions that cause ply-movement during manufacturing using 3D Digital Image Correlation (DIC). We quantify the interfacial ply-movement during the composite processing to cure cycle, thereby observe the formation of defects. Here we focus on the lateral movement of plies that leads to the formation of wrinkles.

2. EXPERIMENTAL SETUP

The new experimental approach devised in this paper uses a high temperature/pressure autoclave (from ASC systems), instrumented with 3D digital image correlation (DIC) to measure the surface ply deformations and strain during the composite processing. The autoclave is equipped with a borosilicate glass viewport and a light, which enables this measurement while the autoclave is operating on a cure cycle (typically 120 C and 100 psi pressure) for composite fabrication. The DIC system from Correlated Solutions has two 6-megapixel high-resolution cameras and is capable of measuring both in-plane and out of plane displacements and strains. Figure 2 shows the autoclave with the camera setup. A speckle pattern is spray-painted on to the specimen. The DIC is then used to capture timed pictures of the specimen during a cure. The relative movement of the speckle pattern is analyzed in VIC-3D software to determine surface displacements and strains. Results indicate that in the case of prepreg composites these surface displacements are directly correlated to the kinematics of ply interfaces.

While there have been some methods for in-situ monitoring during processing that use embedded piezoceramics [24], fiber Bragg grating sensors [25] or fiber optic sensors [26], these are often limited to discrete points and alter the structure of the material, the in-situ monitoring approach used in this research provides spatially and temporally continuous data and does not modify the fibers or matrix, therefore does not alter the thermomechanical properties. Moreover, this approach is based on a pressurized autoclave, which is the preferred manufacturing environment for composites, therefore the understanding developed here can be translated to practice more readily.

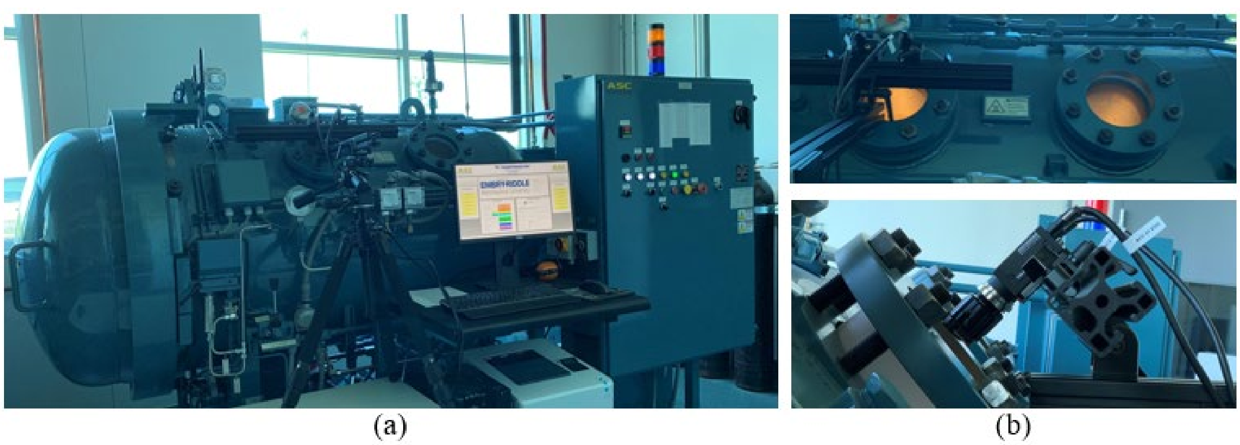

Figure 2. (a) Autoclave with 3D DIC. (b) Autoclave viewports and DIC cameras.

Composite specimens of dimensions 20.32x15.24x10^{-2} m (8"x6") are prepared for fabrication using four $[90/90]_s$ oriented plies of unidirectional carbon fiber prepreg from Fibre Glast

Corporation. A white speckle pattern is sprayed on the top layer of the layup as shown in figure 3(c) for creating high contrast, random speckle pattern for digital image correlation. The layup and the tool configuration using cylindrical tools of three diameters in this research are designed to maximize the inter ply-movement as shown in the schematic in figure 3(a). The plies are laid upon these three molds and prepared for curing as seen in figure 3(b). The cure cycle by Fibre Glast consists of a ramp up and ramp down temperatures of less than 5ºC per min to a target temperature of 120 ºC at 690 kpa pressure. The hold time of 1hr along with other parameters was programmed into the autoclave composite processing control (CPC).

(a) (b) (c)

Figure 3. (a): Schematic of layup; (b) Layup over the cylindrical tool; (c) Specimen after cure.

After transferring the layup to the autoclave, the DIC cameras are set up pointing at the composite layup inside the autoclave through the viewport as shown in figure 2 (b). Both the autoclave cure cycle and the camera system are started at the same time capturing pictures throughout the cure cycle. Due to the ply-movement, the relative movement in the speckles on the top layer of the layup is analyzed in VIC-3D software to determine surface displacements and strains as shown in figure 4 (a). The results of this experimental approach provide an insight into the interfacial motion between plies resulting in surface deformations like wrinkles Further, it will lead to the quantification of the process conditions (temperature, pressure, cure cycle) and the tool geometry that lead to the movement of plies and manufacturing defects.

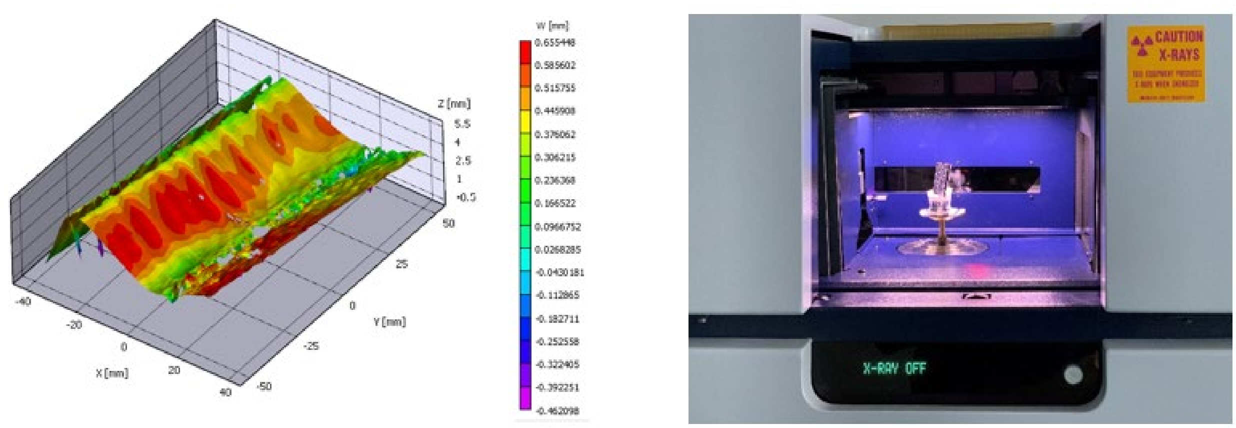

(a) (b)

Figure 4. (a): DIC VIC-3D analysis capturing wrinkles; (b) Specimen installed in X-ray

The interfacial kinematics and the related defect formation post-curing will be validated and characterized using SkyScan 1275 Desktop X-ray Microtomograph from Bruker. Due to the sample size limitations of this X-ray machine, a new small specimen of dimensions 5.08x3.81x10-2 m (2"x1.5") was taken from the original specimen. After installing the sample in the SkyScan as shown in figure 4 (b), X-ray energy of 100kV is used to scan the samples from different angles. The scan is then reconstructed using NRecon software to get the full structural detail of the specimen. A variety of problems in materials research [27] applied X-ray Micro-CT with a few recent studies reporting on polymer matrix composites [28,29]. X-ray Micro-CT in this research will provide a 3D structural detail post-curing to correlate with the in-situ interface movement measurements obtained during the processing.

3. RESULTS AND DISCUSSION

The pictures obtained from the DIC cameras for three different molds are analyzed in VIC-3D software for change in displacements in the out-of-plane Z direction. These displacements are the result of the interfacial ply movement happening due to the combination of the thermomechanical loads during the cure as well as residual stresses generated due to the crosslinking of the polymer bonds [24]. The average out of plane (Z) displacement at the end of the cure and the maximum displacement at a wrinkle in Z-direction are plotted in figure 5. Shrinkage can be observed in figure 5 (a) with an average displacement of $-0.058\text{x}10^{-3}$ m is observed for mold with a 9.5mm radius and $-0.046\text{x}10^{-3}$ m is observed for mold with 12.7mm diameter cylindrical tool. Even after shrinkage, the average out of plane displacement for mold with 15.9mm diameter is $0.005\text{x}10^{-3}$ m due to wrinkles affecting the average.

After the ramp-up stage of cure cycle and gelation, the interfacial ply slippage next to the cylindrical tool slowly increases eventually forming wrinkles towards the end of processing. Figure 5 (b) shows the height of the biggest wrinkle developed for all three molds. For the mold with a cylindrical tool of diameter 9.5mm, the biggest wrinkle is measured to be $0.54\text{x}10^{-3}$ m. For diameter 12.7mm, the wrinkle height is measured at $0.81\text{x}10^{-3}$ m and the biggest wrinkle of all is measured at $1.32\text{x}10^{-3}$ m for mold with a cylindrical tool of diameter 15.9mm. These results show a pattern of higher ply-movement for mold with higher curvature resulting in the biggest wrinkle observed for mold with a cylindrical diameter of 15.9mm.

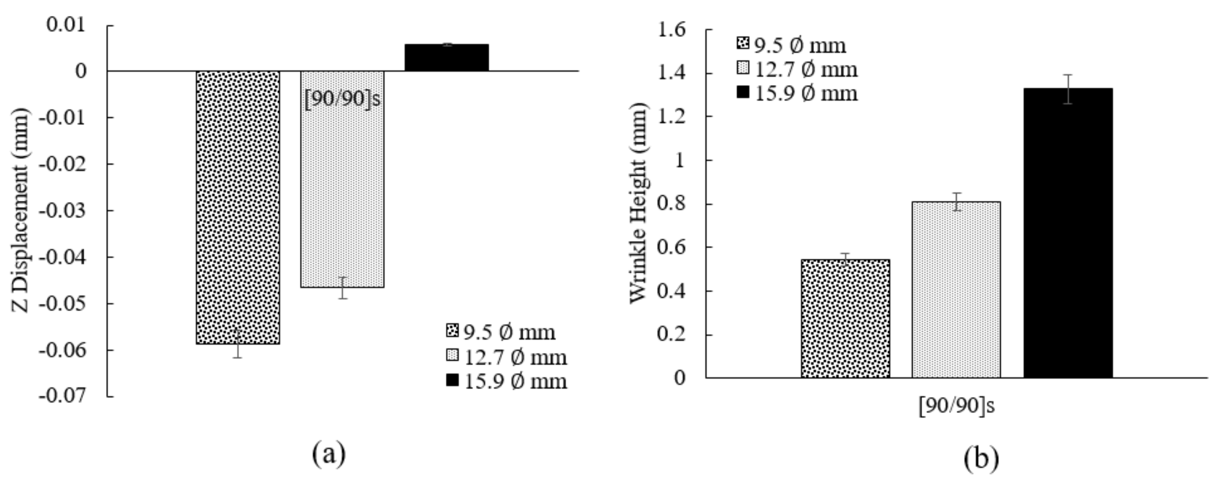

Figure 5. (a) Average out of plane displacement; (b) Biggest wrinkle height.

Along with mechanisms like buckling of fibers [30], internal residual stresses [31] and shear between plies [32], the effect of cure cycle [33], tool geometry [34], part geometry [35] and layup orientation of the plies [36] also play a key role in the formation of wrinkles and delamination. Fernlund et al. [37] conducted experiments to understand the effect of tool geometry and curing parameters on L and C shaped composite parts observing that high CTE tooling material gives C-shaped parts more spring-in than L-shaped parts. They also found that thin parts have more spring-in than thick parts. Tool-part geometry is highly considered in creating the mold used in this paper to elevate the effect of curvature on the ply movement. Pandey and Sun [38] analyzed the mechanisms of wrinkle formation during the processing of continuous-fiber polymeric composites and found out that wrinkling is triggered by the buckling of one layer experiencing maximum compression. They observed that the other layers in the layup provide support to the unwrinkled part of the wrinkling layer. This analysis also supports the experiments conducted in this paper creating three different compression forces on the same layup with three different curvatures of the mold.

X-ray Micro-CT has been utilized in the literature to characterize various features in materials research including fracture [39], fiber breakage [40], porosity [41], and crack growth [42] along with fiber waviness [43]. Almost all of these studies are for metal-matrix composites but in this paper, it is applied to polymer matrix composites. Figure 6 shows the 3D reconstruction of the sample from X-ray Micro-CT with figure 6(a) showing wrinkles on the top surface along with internal delaminations. The length of the wrinkle measured from X-ray as shown in figure 6(b), internal sectional view, is 1.32×10^{-3} m, which is the same as the out-of-plane displacement at biggest wrinkle measured from the DIC (figure 6) at the end of the cure. This independent ex-situ measurement validates the in-situ experimental approach.

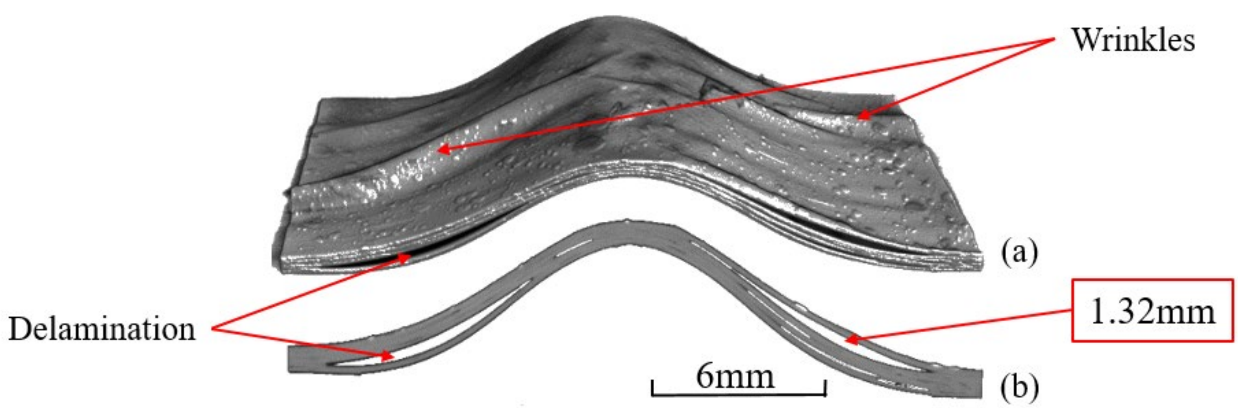

Figure 6. X-ray Micro-CT showing surface wrinkles & internal delamination

Various modeling techniques have been used in the past to model wrinkles and delamination. Zhu et al. [44] used theoretical modeling to model shear deformation and wrinkling of a plain-woven composite. They formulated mathematical expressions to predict the shear energy and critical shear angle of composite fabrics. Hasiao and Daniel [45] developed an analytical model for investigating the effects of fiber waviness on stiffness and strength of unidirectional composites under compressive loading. In their research, they modeled uniform, graded and localized waviness patterns. Slippage coefficient [46], Reynolds equation [47] and power-law approximations [48] are a few other methods used in the literature to model interply adhesion and ply slippage. While these models effectively identified the effects of fiber wrinkling and delamination, the in-situ capability presented in this paper can quantitatively identify the formation of wrinkles during the processing of composites. From figure 6 it is evident that there are wrinkles formed on the specimen after cure and from figure 5 it is also observed that curvature of the tool/part geometry plays a key role in the generation of bigger wrinkles and higher delamination. The experimental approach developed in this research can be utilized to understand how various processing parameters affect the manufacturing of composite parts and approaches can be devised to adjust these parameters to minimize processing induced defects like wrinkles and delaminations.

4. SUMMARY

In summary, a total of three mold configurations were developed using three different diameter cylindrical tools. Composite samples were prepared by curing a four-ply layup upon these mold configurations in an autoclave with viewports. Digital Image Correlation (DIC) cameras are set up through the viewports to capture and measure the out-of-plane ply movement. Resulting defects wrinkles and delamination are characterized post-cure through X-ray Micro-CT. The research approach used in this paper can be used to understand the evolution of composite manufacturing defects like wrinkles and delamination and device approaches to reduce these defects.

Acknowledgment

The financial support from ERAU internal grant is gratefully acknowledged.

5. REFERENCES

1. Marsh, G. (2005). Airframers exploit composites in battle for supremacy. Reinforced plastics, 49(3), 26-32. https://doi.org/10.1016/S0034-3617(05)00577-1
2. Witik, R. A., Payet, J., Michaud, V., Ludwig, C., & Månson, J. A. E. (2011). Assessing the life cycle costs and environmental performance of lightweight materials in automobile applications. Composites Part A: Applied Science and Manufacturing, 42(11), 1694-1709. https://doi.org/10.1016/j.compositesa.2011.07.024
3. Nanni, A. (1993). FRP reinforcement for prestressed and non-prestressed concrete structures. In Fiber-Reinforced-Plastic (FRP) Reinforcement for Concrete Structures (pp. 3-12). Elsevier https://doi.org/10.1016/B978-0-444-89689-6.50005-7
4. Sutton, A. P. (1995). Interfaces in crystalline materials. Monographs on the Physice and Chemistry of Materials, 414-423.
5. Sanchez, I. C. (Ed.). (2013). Physics of polymer surfaces and interfaces. Butterworth-Heinemann.
6. Plueddemann, E. P. (Ed.). (2016). Interfaces in Polymer Matrix Composites: Composite Materials (Vol. 6). Elsevier.
7. Greszczuk, L. (1969). Theoretical studies of the mechanics of the fiber-matrix interface in composites. In Interfaces in composites. ASTM International. https://doi.org/10.1520/STP44699S
8. Hsueh, C. H. (1990). Interfacial debonding and fiber pull-out stresses of fiber-reinforced composites. Materials Science and Engineering: A, 123(1), 1-11. https://doi.org/10.1016/0921-5093(90)90203-F

9. Chandra, N., Li, H., Shet, C., & Ghonem, H. (2002). Some issues in the application of cohesive zone models for metal–ceramic interfaces. International Journal of Solids and Structures, 39(10), 2827-2855. https://doi.org/10.1016/S0020-7683(02)00149-X
10. Smith, R. A. "Composite defects and their detection." Materials science and engineering 3 (2009): 103-143.
11. Petrescu, R.V., Aversa, R., Akash, B., Corchado, J., Berto, F., Apicella, A. and Petrescu, F.I., "When boeing is dreaming–a review", 2017. https://doi.org/10.3844/jastsp.2017.149.161
12. Heslehurst, Rikard Benton. "Defects and damage in composite materials and structures", CRC Press, 2014. https://doi.org/10.1201/b16765
13. Allaoui, S., Hivet, G., Soulat, D., Wendling, A., Ouagne, P. and Chatel, S., "Experimental preforming of highly double curved shapes with a case corner using an interlock reinforcement". International Journal of Material Forming 7(2), (2014), pp.155-165.. https://doi.org/10.1007/s12289-012-1116-5
14. Tallinen, T., Ojajärvi, J., Åström, J. A., & Timonen, J. (2010). Scaling behavior in non-hookean compression of thin-walled structures. Physical review letters, 105(6), 066102. https://doi.org/10.1103/PhysRevLett.105.066102
15. Prodromou, A. G., & Chen, J. (1997). On the relationship between shear angle and wrinkling of textile composite preforms. Composites Part A: Applied Science and Manufacturing, 28(5), 491-503. https://doi.org/10.1016/S1359-835X(96)00150-9
16. Zhu, B., Yu, T. X., & Tao, X. M. (2007). An experimental study of in-plane large shear deformation of woven fabric composite. Composites Science and Technology, 67(2), 252-261. https://doi.org/10.1016/j.compscitech.2006.08.011
17. Pandey, R. K., & Sun, C. T. (1999). Mechanisms of wrinkle formation during the processing of composite laminates. Composites science and technology, 59(3), 405-417. https://doi.org/10.1016/S0266-3538(98)00080-3
18. Fish, J., LeMonds, J., & Shek, K. L. (1999). Modeling of wrinkling in compression molding of composites. Journal of engineering mechanics, 125(8), 951-955. https://doi.org/10.1061/(ASCE)0733-9399(1999)125:8(951)
19. Dodwell, T. J., Butler, R., & Hunt, G. W. (2014). Out-of-plane ply wrinkling defects during consolidation over an external radius. Composites Science and Technology, 105, 151-159. https://doi.org/10.1016/j.compscitech.2014.10.007
20. Erland, S., Dodwell, T. J., & Butler, R. (2014). Inter and intra-ply shearing of uncured carbon fibre laminates. In ECCM16-16TH European Conference on Composite Materials, June(pp. 22-26).
21. Croft, K., Lessard, L., Pasini, D., Hojjati, M., Chen, J. and Yousefpour, A. "Experimental study of the effect of automated fiber placement induced defects on performance of composite laminates". Composites Part A: Applied Science and Manufacturing, 42(5), (2011), pp.484-491. https://doi.org/10.1016/j.compositesa.2011.01.007
22. Meola, C. and Carlomagno, G.M., "Infrared thermography to evaluate impact damage in glass/epoxy with manufacturing defects". International Journal of Impact Engineering 67, (2014): pp.1-11. https://doi.org/10.1016/j.ijimpeng.2013.12.010
23. Yin, H., Peng, X., Du, T. and Guo, Z., "Draping of plain woven carbon fabrics over a double-curvature mold". Composites Science and Technology, 92, (2014): pp.64-69. https://doi.org/10.1016/j.compscitech.2013.12.013

24. Lin, M., & Chang, F. K. (2002). The manufacture of composite structures with a built-in network of piezoceramics. Composites Science and Technology, 62(7-8), 919-939. https://doi.org/10.1016/S0266-3538(02)00007-6
25. Kuang, K., Kenny, R., Whelan, M. P., Cantwell, W. J., & Chalker, P. R. (2001). Embedded fibre Bragg grating sensors in advanced composite materials. Composites Science and Technology, 61(10), 1379-1387. https://doi.org/10.1016/S0266-3538(01)00037-9
26. Crosby, P. A., Powell, G. R., Fernando, G. F., France, C. M., Spooncer, R. C., & Waters, D. N. (1996). In situ cure monitoring of epoxy resins using optical fibre sensors. Smart materials and structures, 5(4), 415. https://doi.org/10.1088/0964-1726/5/4/005
27. Stock, S. R. "X-ray microtomography of materials." International Materials Reviews 44.4 (1999): 141-164. https://doi.org/10.1179/095066099101528261
28. Croom, B., Wang, W.M., Li, J. and Li, X., "Unveiling 3D deformations in polymer composites by coupled micro x-ray computed tomography and volumetric digital image correlation". Experimental Mechanics, 56(6), (2016): pp.999-1016. https://doi.org/10.1007/s11340-016-0140-7
29. Senck, S., Scheerer, M., Revol, V., Dobes, K., Plank, B. and Kastner, J., "Non-destructive evaluation of defects in polymer matrix composites for aerospace applications using x-ray Talbot-Lau interferometry and micro CT". 58th AIAA/ASCE/AHS/ASC Structures, Structural Dynamics, and Materials Conference, 2017, (p. 0355). https://doi.org/10.2514/6.2017-0355
30. Potter, K. D. "Understanding the origins of defects and variability in composites manufacture." International Conference on Composite Materials (ICCM)-17, Edinburgh, UK. 2009.
31. Breuer, U., Neitzel, M., Ketzer, V. and Reinicke, R., "Deep drawing of fabric-reinforced thermoplastics: Wrinkle formation and their reduction". Polymer composites, 17(4), (1996): pp.643-647. https://doi.org/10.1002/pc.10655
32. Hallander, P., Akermo, M., Mattei, C., Petersson, M. and Nyman, T., "An experimental study of mechanisms behind wrinkle development during forming of composite laminates". Composites Part A: Applied Science and Manufacturing, 50, (2013): pp.54-64. https://doi.org/10.1016/j.compositesa.2013.03.013
33. Liu, L., Zhang, B. M., Wang, D. F., & Wu, Z. J. Effects of cure cycles on void content and mechanical properties of composite laminates. Composite structures, 73(3), (2006) 303-309. https://doi.org/10.1016/j.compstruct.2005.02.001
34. Haddad, M., Zitoune, R., Eyma, F., & Castanie, B. Study of the surface defects and dust generated during trimming of CFRP: Influence of tool geometry, machining parameters and cutting speed range. Composites Part A: Applied Science and Manufacturing, 66, (2014) 142-154. https://doi.org/10.1016/j.compositesa.2014.07.005
35. De Moura, M. F. S. F., Daniaud, R., & Magalhaes, A. G. Simulation of mechanical behaviour of composite bonded joints containing strip defects. International journal of adhesion and adhesives, 26(6), (2006) 464-473. https://doi.org/10.1016/j.ijadhadh.2005.06.010
36. Lightfoot, J. S., Wisnom, M. R., & Potter, K. Defects in woven preforms: Formation mechanisms and the effects of laminate design and layup protocol. Composites Part A: Applied Science and Manufacturing, 51, (2013) 99-107. https://doi.org/10.1016/j.compositesa.2013.04.004

37. Fernlund, G., Rahman, N., Courdji, R., Bresslauer, M., Poursartip, A., Willden, K., & Nelson, K. Experimental and numerical study of the effect of cure cycle, tool surface, geometry, and lay-up on the dimensional fidelity of autoclave-processed composite parts. Composites part A: applied science and manufacturing, 33(3), (2002) 341-351. https://doi.org/10.1016/S1359-835X(01)00123-3
38. Pandey, R. K., & Sun, C. T. Mechanisms of wrinkle formation during the processing of composite laminates. Composites science and technology, 59(3), (1999) 405-417. https://doi.org/10.1016/S0266-3538(98)00080-3
39. Borbély, A., Biermann, H., Hartmann, O., & Buffière, J. Y. The influence of the free surface on the fracture of alumina particles in an Al–Al2O3 metal–matrix composite. Computational materials science, 26, (2003) 183-188. https://doi.org/10.1016/S0927-0256(02)00397-X
40. Maire, E., Babout, L., Buffiere, J. Y., & Fougeres, R. Recent results on 3D characterisation of microstructure and damage of metal matrix composites and a metallic foam using X-ray tomography. Materials Science and Engineering: A, 319, (2001) 216-219. https://doi.org/10.1016/S0921-5093(01)00924-8
41. Mummery, P. M., Derby, B., Anderson, P., Davis, G. R., & Elliott, J. C. X-ray microtomographic studies of metal matrix composites using laboratory X-ray sources. Journal of Microscopy, 177(3), (1995) 399-406. https://doi.org/10.1111/j.1365-2818.1995.tb03570.x
42. McDonald, S. A., Preuss, M., Maire, E., Buffiere, J. Y., Mummery, P. M., & Withers, P. J. X-ray tomographic imaging of Ti/SiC composites. Journal of microscopy, 209(2), (2003) 102-112. https://doi.org/10.1046/j.1365-2818.2003.01105.x
43. Baaklini, G. Y., Bhatt, R. T., Eckel, A. J., Engler, P., Rauser, R. W., & Castelli, M. G. X-ray microtomography of ceramic and metal matrix composites. Materials evaluation, 53(9) (1995).
44. Zhu, B., Yu, T. X., Teng, J., & Tao, X. M. Theoretical modeling of large shear deformation and wrinkling of plain woven composite. Journal of Composite Materials, 43(2), (2009) 125-138. https://doi.org/10.1177/0021998308098237
45. Hsiao, H. M., & Daniel, I. M. Effect of fiber waviness on stiffness and strength reduction of unidirectional composites under compressive loading. Composites science and technology, 56(5), (1996) 581-593. https://doi.org/10.1016/0266-3538(96)00045-0
46. Cho, M., Kim, M.H., Choi, H.S., Chung, C.H., Ahn, K.J. and Eom, Y.S., “A study on the room-temperature curvature shapes of unsymmetric laminates including slippage effects”. Journal of composite materials, 32(5), (1998): pp.460-482. https://doi.org/10.1177/002199839803200503
47. Hanna, E.G., Poitou, A. and Casari, P., “MODELING THE INTERPLY SLIP DURING FORMING OF THERMOPLASTIC LAMINATES”. Materials Physics and Mechanics, 40, (2018): pp.22-36.
48. Morris, S.R. and Sun, C.T., “An investigation of interply slip behaviour in AS4/PEEK at forming temperatures”. Composites Manufacturing, 5(4), (1994): pp.217-224. https://doi.org/10.1016/0956-7143(94)90136-8